




Structural role in temperature-induced magnetization reversal revealed in distorted perovskite $\text{Gd}_{1-x}\text{Y}_x\text{CrO}_3$

Pooja Jain ^{1,2} Shivani Sharma,³ Ryan Baumbach,⁴ Arvind Kumar Yogi ¹, I. Ishant,⁵ M. Majumder,⁵ Theo Siegrist,^{3,6} M. K. Chattopadhyay ^{7,8} and N. P. Lalla^{1,*}

¹UGC-DAE Consortium for Scientific Research, Indore-452001, India

²Government Adarsh College Jhabua, Ratanpura, Jhabua-457661, India

³National High Magnetic Field Laboratory, Florida State University, Tallahassee, Florida 32310, USA

⁴Department of Physics, Florida State University, Tallahassee, Florida 32310, USA

⁵Department of Physics, Shiv Nadar Institution of Eminence, Gautam Buddha Nagar 201314, Uttar Pradesh, India

⁶Department of Chemical and Biomedical Engineering, FAMU-FSU College of Engineering, Tallahassee, Florida 32310, USA

⁷Free Electron Laser Utilization Laboratory, Raja Ramanna Centre for Advanced Technology, Indore-452013, India

⁸Homi Bhabha National Institute, Training School Complex, Anusakti Nagar, Mumbai 400094, India



(Received 9 September 2023; revised 11 January 2024; accepted 20 February 2024; published 8 March 2024)

The phenomenon of temperature induced magnetization-reversal, giving rise to negative magnetization (NM) in several rare-earth chromates, has been revisited through magnetization studies on $\text{Gd}_{1-x}\text{Y}_x\text{CrO}_3$. The study re-examines the well accepted explanation of NM, i.e., the antiparallel polarization of the paramagnetic rare-earth (R^{3+}) moments against the weak magnetization (M_{Cr}) of the canted antiferromagnetically ordered Cr^{3+} moment subsystem and compares the results with a relatively new explanation invoking frustration of the Gd^{3+} moment subsystem at temperatures as high as 170 K [Phys. Rev. B **99**, 014422 (2019)]. Keeping in view the highly localized nature of f electrons the invoked frustration appears unphysical. We find that the magnitude of the NM increases with increasing concentration of nonmagnetic Y^{3+} ion. This is attributed to increased antiparallel polarization of the Gd^{3+} moments against increased M_{Cr} , due to structural modifications in $\text{Gd}_{1-x}\text{Y}_x\text{CrO}_3$ with increasing Y^{3+} content. This observation strongly contradicts the interpretation for NM based on the frustration of Gd^{3+} moments. The temperature induced negative to positive magnetization jump (TMJ) is observed and is attributed to the minimization of the Zeeman-energy against an energy barrier. A phenomenological comparative study of the modified Curie-Weiss fitting to $M(T)$ indicates that TMJ in polycrystalline $\text{Gd}_{1-x}\text{Y}_x\text{CrO}_3$ is an outcome of cascaded individual flips of Gd^{3+} moments occurring over random sites having homogeneously distributed barrier energy. In our analysis the $M(T)$ data is fitted using modified Curie-Weiss treating M_{Cr} to be temperature dependent, i.e., $M_{\text{Cr}}(T) = M(0) \cdot [1 - (T/T_C)^\alpha]^\beta$.

DOI: [10.1103/PhysRevB.109.094410](https://doi.org/10.1103/PhysRevB.109.094410)

I. INTRODUCTION

In the recent past the rare-earth (RE) and transition-metal based magnetic distorted perovskites, like orthomanganites (REMnO_3) [1–3] and orthoferrites (REFeO_3) [4] have been intensively studied due to their magnetoelectric multiferroic properties, which have immense potential for technological applications. The coexistence of highly localized rare-earth (RE) f -electron moments, which are known to very weakly interact and order at very low-temperatures, and the $3d$ -transition metal moments, which strongly interact and order at relatively high-temperatures, bring out a variety of interesting physics. In the same series, the RE orthochromites (RECrO_3) are found to be particularly interesting due to their coexisting functionalities comprising multiferroicity [5–7], spin-reorientation phase-transition (SRPT) [8–10] and magnetization-reversal [11–18], which has the potential for novel applications in fast magnetic switching devices [19–21] including laser-induced ultrafast spin-reorientation, spintronics [22] and magnetic refrigeration [23]. The remarkable

properties in these compounds arise out of the polarizability of the RE^{3+} moments under the internal field of Cr^{3+} moments, which order due to their antisymmetric superexchange leading to Dzyaloshinskii-Moriya (DM) interaction [24,25]. Here we revisit the occurrence of negative magnetization (NM) in RECrO_3 compounds [10,14,26–39].

The presence of two types of magnetic ions, namely partially filled $4f$ shell RE^{3+} cations and $3d$ shell Cr^{3+} cations, in RECrO_3 orthochromates with $Pbnm$ space group, play an important role in its magnetic states. The possible magnetic interactions are namely $\text{Cr}^{3+} - \text{Cr}^{3+}$, $\text{Cr}^{3+} - \text{RE}^{3+}$ and $\text{RE}^{3+} - \text{RE}^{3+}$, which consist of isotropic, the antisymmetric, and the anisotropic-symmetric superexchange interactions. With decreasing temperature, a canted antiferromagnetic (CAFM) ordering of the Cr^{3+} moments takes place at relatively high-temperatures, e.g. in GdCrO_3 $T_{\text{N}1} = 170$ K. However, at and below $T_{\text{N}1} = 170$ K the RE^{3+} moments remain paramagnet and order only below 5–10 K. RECrO_3 compounds undergo SRPT at low temperatures due to the rotation of its easy axis of magnetization from the \mathbf{a} to the \mathbf{c} direction [27].

In its paramagnetic state the RE^{3+} moments feel the molecular field (Weiss-field) of the ordered Cr^{3+} moment subsystem

*Corresponding author: nplallaiuc82@gmail.com

and get partially magnetized (polarized). Below the CAFM transition temperature T_{N1} , a few of the RECrO_3 orthochromates show NM. The observed NM is completely different from the diamagnetic state. Here the differential susceptibility (dM/dH) remains positive [15,16]. But in orthovanadates, and some spinel compounds, there are other specific reasons causing NM. For example in YVO_3 [40], a competition between single-ion magnetic anisotropy and the antisymmetric Dzyaloshinsky-Moriya interaction lead to NM [24,25].

As described above, the physics of NM, observed in magnetic rare-earth chromates (RCrO_3) based orthorhombic distorted perovskites, was thought to be rather well understood and well accepted. However, the study on GdCrO_3 by Tripathi *et al.* [26] in 2019, gives a totally new interpretation of this phenomena. They attributed it to the frustration of Gd moments. They used neutron scattering, and keeping in view the high neutron absorption coefficient of Gd they used high energy neutrons with wavelength $\sim 0.5 \text{ \AA}$. Although this was an innovative approach, the use of shorter wavelength decreased the resolution of the scattering data by \sim four times *w.r.t.* to the usual practice of using larger wavelengths of $\sim 2.2 \text{ \AA}$ at most of the neutron beam lines for probing magnetic structures. Due to the poor resolution of the neutron data, the extractability of proper magnetic structure is very much likely to be compromised leading the unphysical conclusion of the existence of magnetically frustrated Gd-Gd correlation, claimed to exist at temperatures as high as 170 K. However, given that the Gd-Gd magnetic interaction is likely to be very weak, the conjecture that it is frustrated at temperatures as high as $\sim 170 \text{ K}$ is unreasonable

Keeping in view the issues with Gd containing samples, the neutron scattering approach to understand NM in GdCrO_3 is most likely to be inconclusive. However, the effect of Gd-Gd frustrated correlation [26], if at all present in GdCrO_3 , can be distinctly investigated through substitution of nonmagnetic rare-earth ions, e.g., Y^{3+} , at the Gd site. As asserted in Ref. [26], if the Gd-Gd correlation is at all frustrated and responsible for the NM in GdCrO_3 , then with increasing Y^{3+} content the NM effect should have minimized. Contrary to this, our magnetization study on a series of $\text{Gd}_{1-x}\text{Y}_x\text{CrO}_3$ compound clearly shows an in general increase in NM with increasing Y^{3+} content. Our findings argue against the interpretation of NM as given in Ref. [26]. Our data gets fully and physically accounted for by the theory of antiparallel polarization of RE^{3+} ions against the uncompensated moment of the CAFM ordered Cr^{3+} moments. It shows the presence of polarizability of the Gd^{3+} moments even in its highly diluted condition for $x = 0.9$.

II. EXPERIMENTAL

Polycrystalline samples of $\text{Gd}_{1-x}\text{Y}_x\text{CrO}_3$ ($x=0, 0.10, 0.25, 0.40, 0.50, 0.67, 0.75, 0.80, 0.90, \text{ and } 1.00$) were prepared via solid-state reaction route using 99.99% pure ingredients of Gd_2O_3 , Y_2O_3 , and Cr_2O_3 . The stoichiometric mixture of well dried ingredients was thoroughly ground for about 8 hrs using an agate mortar pestle. The mixture was then calcined at 1200°C for 12 h. The calcined powder was reground, pelletized and sintered at 1450°C for 24 h. The as synthesized samples were subjected to powder x-ray diffraction (XRD)

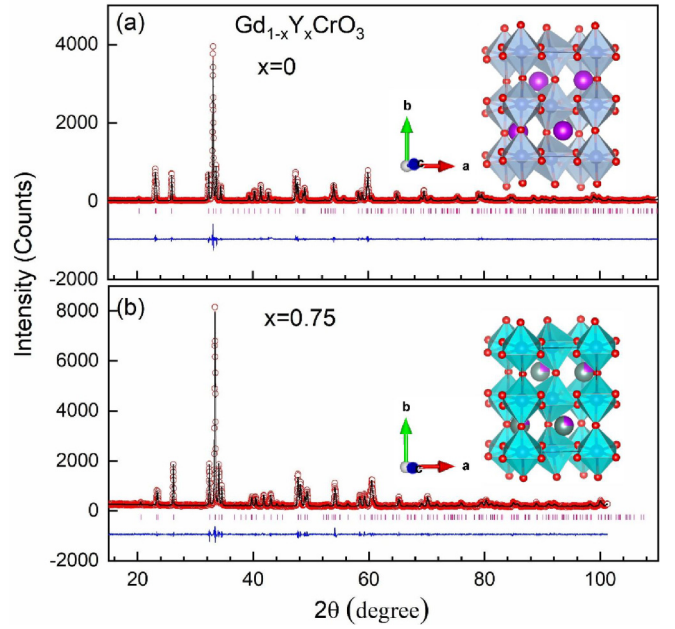


FIG. 1. RT-XRD patterns of $\text{Gd}_{1-x}\text{Y}_x\text{CrO}_3$ for (a) $x = 0$ and (b) $x = 0.75$. Its Rietveld refinement using $Pbmm$ space-group shows absence of any unaccounted peak confirming to the formation of single phase samples. Rietveld refined RT-XRD patterns corresponding to all the studied compositions of $\text{Gd}_{1-x}\text{Y}_x\text{CrO}_3$ are given in the SM [42].

for structural and phase purity characterizations. The XRD experiments were performed using a Huber θ - 2θ diffractometer equipped with a graphite (002) monochromator. The well characterized samples were subjected to magnetization studies. Magnetization $M(T)$ as function of temperature, was measured with a rate of 0.5 K/min under zero-field cooled (ZFC), field cooled cooling (FCC) and field cool warming (FCW) protocols at 500 Oe using MPMS-3 SQUID VSM (superconducting quantum-interference device based vibrating sample magnetometer) of QD, USA made.

III. RESULTS AND DISCUSSIONS

A. Structural studies

Powder XRD patterns of all the studied compositions were Rietveld refined using the $Pbmm$ space-group. Refinements were done using Jana 2006 software [41]. Figures 1(a) and 1(b) present typical example of Rietveld refined RT-XRD patterns of $\text{Gd}_{1-x}\text{Y}_x\text{CrO}_3$ (for $x = 0$ and 0.75). The insets show the crystal structure models drawn using VESTA based on the refined Wyckoff positions. The refined RT-XRD patterns of all the studied samples are presented in Fig. SM1, see the Supplemental Material (SM) [42]. The absence of any unaccounted peak confirms the single-phase nature of the samples. The refined crystal structure parameters and the Wyckoff positions of $\text{Gd}_{1-x}\text{Y}_x\text{CrO}_3$ with different x are presented in Table SM1 [42]. Figure 2 graphically shows the Y^{3+} concentration dependence of the unit-cell parameters and the Cr-O2-Cr bond-angle. It can be seen that Cr-O2-Cr bond angle, spanning in the ab plane, decreases monotonically right from $x = 0$. The decrease in the lattice parameters is attributed

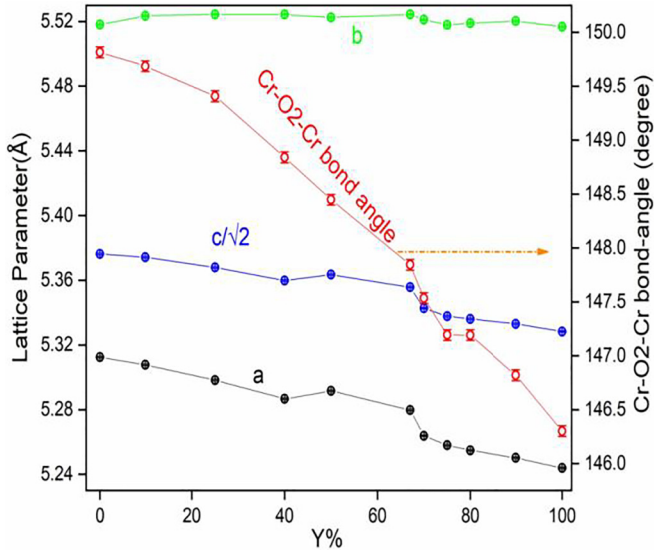


FIG. 2. Y^{3+} concentrations (x) dependence of the lattice parameters, and Cr-O2-Cr bond angle of $Gd_{1-x}Y_xCrO_3$ with $Pbnm$ structure.

to the smaller size Y^{3+} (1.019 Å) ion at the Gd^{3+} (1.053 Å) A site in a VIII coordination polyhedral environment [43]. Substitution of a smaller size ion at the A site in an ABO_3 perovskite is likely to increase the tilt of the BO_6 octahedra and hence decrease the Cr-O2-Cr bond angle [44]. Y^{3+} concentration dependence of the Cr-O-Cr bond angles measured both along the c axis and in the ab plane is listed in Table SM2 [42]. In the following we show the correlation between the Cr-O2-Cr bond angle and various other features of the $M(T)$ variation.

B. Magnetization studies

$GdCrO_3$ undergoes two magnetic transitions, CAFM at $T_{N1} = 172$ K and SRPT immediately followed by Gd^{3+} moment ordering at ~ 4 K [5,8,16,17,26]. Within the $Gd_{1-x}Y_xCrO_3$ series, diluting the concentration of high magnetic moment ion Gd^{3+} by a nonmagnetic ion Y^{3+} , is expected to show some interesting magnetization features. The temperature dependent ZFC, FCC, and FCW $M(T)$ s measured under 500 Oe are shown in Fig. SM2 [42]. Like previous reports [16,17,26] these $M(T)$ s show systematic occurrence of temperature induced NM. The enlarged view of these $M(T)$ s are presented here in Figs. 3(a)–3(d), which highlights some interesting features appearing as a function of Y^{3+} concentration. The CAFM transition temperature T_{N1} gradually decreases with Y^{3+} content. Other features of FCC- $M(T)$ s like compensation temperatures T_{comp1} and T_{comp2} , show similarity with the earlier studies on pristine $GdCrO_3$ [16,17,26]. Figures 3(a)–3(d) show that below CAFM transition the FCC magnetization first reach a plateau like maximum and then crosses zero at T_{comp1} , which shifts to lower values with increasing Y^{3+} content. Below T_{comp1} the FCC- $M(T)$ keeps decreasing with increasingly higher rate, becomes negative and then reaches its minimum ($M_{min-FCC}$) at $T_{min-FCC}$. The negative value of $M_{min-FCC}$ in general increases with increasing Y^{3+} content. These features are summarized in Table SM3

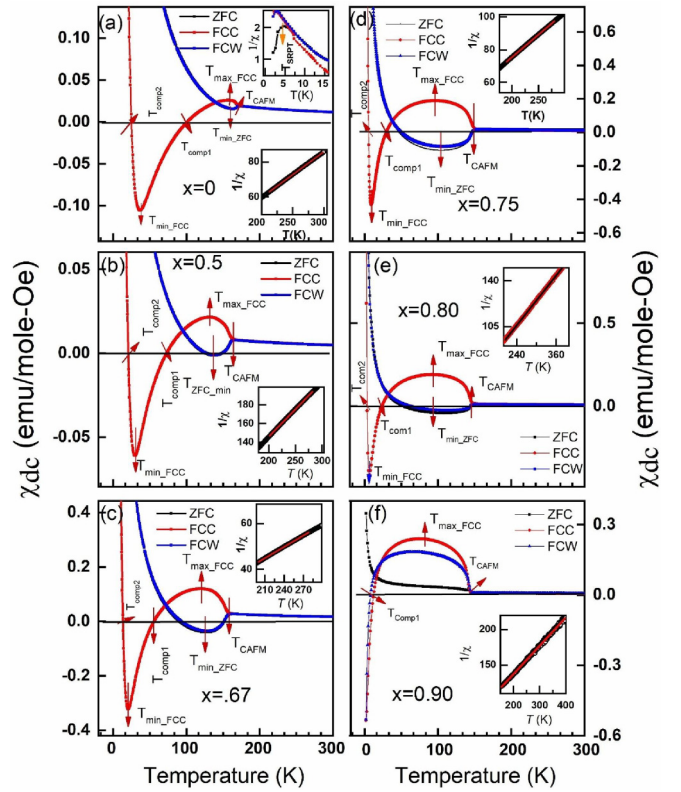


FIG. 3. Enlarged view of the $\chi_{dc}-T$ variations of $Gd_{1-x}Y_xCrO_3$ shown in Fig. 3. It highlights various temperature-wise features of, e.g., T_{comp1} , T_{comp2} , $T_{min-FCC}$, $T_{max-FCC}$, and $T_{min-ZFC}$ and its variation with Y^{3+} concentration ($x = 0 - 0.9$). Unique occurrence of negative magnetization even in the ZFC/FCW $M(T)$ s can also be seen.

in SM and presented graphically in Fig. 4 here. Figure 4(a) shows an unusual feature. Unlike pristine $GdCrO_3$, the minimum of ZFC $M(T)$ ($M_{min-ZFC}$) decreases with Y^{3+} content and becomes negative for $x \geq 0.40$. The corresponding minima temperature, $T_{min-ZFC}$, also decreases with x . Figure 4(b) shows that except for the anomalies at $x = 0.1$ and 0.5 the $M_{min-FCC}$ in general decreases by many folds (> 4 times) with Y^{3+} -content (x). Figure 4(c) shows that the FCC $M(T)$ maxima ($M_{max-FCC}$), appearing just below T_{N1} , shifts to lower temperatures with (x) and has definite correlation with the decreasing Cr-O2-Cr bond angle, however, it has an anomaly at $x = 0.5$. The SRPT has been realized in ZFC $M(T)$ for $x = 0$ (at ~ 4.5 K) and $x = 0.1$ (at ~ 3 K) only.

The occurrence of negative magnetization in magnetic RE orthoferrites (RE)FeO₃ [8] and orthochromates (RE)CrO₃ [10] has been known for quite some time and has been reasonably well explored [11–17] experimentally. In these magnetic rare-earth transition metal (RE)MO₃ perovskites three types of magnetic interactions have been identified, namely $M^{3+} - M^{3+}$, $M^{3+} - R^{3+}$ and $R^{3+} - R^{3+}$. These are generally characterized as the isotropic, the antisymmetric and the anisotropic-symmetric superexchange interactions [10]. The isotropic antisymmetric $M^{3+} - M^{3+}$ superexchange gives rise to the CAFM transition at T_{N1} . Below T_{N1} , due to $M^{3+} - R^{3+}$ superexchange a negative exchange-field appears and as a result the paramagnetic like RE^{3+} ions get AFM polarized (or magnetized) against the uncompensated

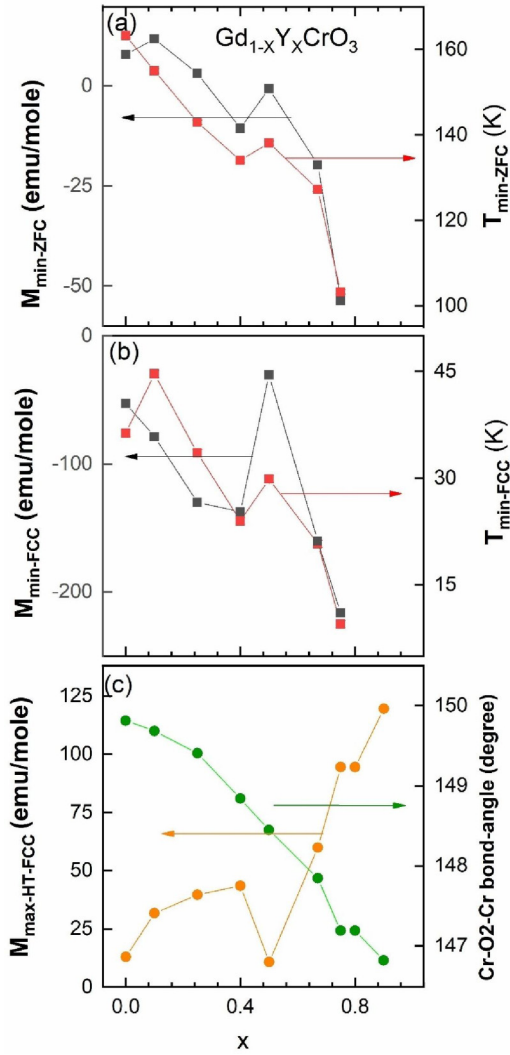


FIG. 4. Graphical presentation of Y³⁺ concentration dependence of some of the features in $M(T)$ variation measured under 500 Oe (a) $M_{\min\text{-ZFC}}$ and $T_{\min\text{-ZFC}}$, (b) $M_{\min\text{-FCC}}$ and $T_{\min\text{-FCC}}$, and (c) $M_{\max\text{-HT-FCC}}$ and Cr-O₂-Cr bond-angle of Gd_{1-x}Y_xCrO₃.

magnetization M_{Cr} . With decreasing temperature, the $M^{3+} - R^{3+}$ interaction thus increases the anisotropy of R^{3+} moments and lead to SRPT. The R^{3+} moments may independently order [35] below the SRPT leading to coexistence of magnetic and polar orders with magnetoelectric coupling [4,27].

The NM of FCC $M(T)$ is well understood in terms of antiparallel polarization of RE^{3+} moments against the uncompensated moments of CAFM ordered Cr^{3+} moments. It is modeled [11,12,16,17] as modified Curie-Wiess law given in the following:

$$M(T) = M_{\text{Cr}} + C(H_{\text{I}} + H)/(T - \theta). \quad (1)$$

Here M_{Cr} , H_{I} , C and θ are the net magnetization due to CAFM ordered Cr^{3+} moments, internal field (or exchange field) experienced by RE^{3+} moments, the Curie constant and the Curie temperature, respectively. H is the external field applied during measurement, which is 500 Oe in the present study. M_{Cr} , H_{I} , and θ are the fitting parameters. The value of C has been estimated for each composition of Gd_{1-x}Y_xCrO₃

and has been kept fixed during fitting iterations. The $M(T)$ data fitted based on Eq. (1) is presented in Figs. SM3(a) and 3(b) [42]. It can be noticed that while the fitting is very good at lower temperatures, it considerably deviates while approaching T_{N1} . Such a discrepancy is seen in other published reports too [11,12,16], but has not been discussed. This discrepancy is due to the fact that the model expressed through Eq. (1) treats M_{Cr} as temperature independent, which is quite unphysical. The CAFM order of the Cr^{3+} moments may be considered to be the summation of two counteracting ferromagnetic (FM) sublattices, which is expected to lead to spontaneous magnetization appearing due to the uncompensated moments of Cr^{3+} . This spontaneous magnetization will most certainly be temperature dependent, and accordingly M_{Cr} , which is expected to be proportional to the spontaneous magnetization, will also be a function of temperature.

For a FM Material, the temperature dependence of spontaneous magnetization (M_{s}), at temperatures $T \rightarrow 0$ K, is due to spin-wave excitations. It is given as Bloch's 3/2 law as,

$$M_{\text{s}}(T) = M_{\text{s}}(0)[1 - (T/T_{\text{C}})^{3/2}]. \quad (2)$$

Additionally, for $T \rightarrow T_{\text{C}}$ it is given as Eq. (3), where β is the critical exponent:

$$M_{\text{s}}(T) = M_{\text{s}}(0)(T_{\text{C}} - T)^{\beta}. \quad (3)$$

Thus the net spontaneous magnetization due to CAFM ordering of Cr^{3+} can be expressed as interpolation of the $M_{\text{Cr}}(T)$ in between 0 K and T_{C} , empirically given [45–47] as Eq. (4):

$$M_{\text{Cr}}(T) = M(0)[1 - (T/T_{\text{N}})^{\alpha}]^{\beta}. \quad (4)$$

Equation (4) has been successfully used to express the temperature dependence of spontaneous magnetization measured using zero-field μ -SR technique and to determine the exponents there in [45–47] to study the nature of the magnetic phase transition.

In view of the above Eq. (1) will get modified to

$$M(T) = M_{\text{Cr}}(T) + C(H_{\text{I}} + H)/(T - \theta). \quad (5)$$

Figures 5 show the FCC and FCW $M(T)$ data for $x = 0, 0.5$, and 0.75 fitted using Eq. (5). The fitted FCC and FCW $M(T)$ data of other compositions are presented in Figures SM 4(a) and 4(b) [42]. It can be noticed that the high-temperature FCC maxima ($M_{\max\text{-FCC}}$) and the FCW/ZFC minima ($M_{\min\text{-FCW}}/M_{\min\text{-ZFC}}$), both are well accounted in these fits. The refined values of the fit parameters are listed in Table I. The values of T_{N1} listed in Table I are exactly the one observed experimentally. Since T_{N1} is a characteristic of the given system, it is kept fixed during fitting iterations.

The occurrence of increasingly high negative $M_{\min\text{-FCC}}$ and positive $M_{\max\text{-FCC}}$ as a function of Y³⁺ content, as depicted in Figs. 4(b) and 4(c), is unusual. Here it becomes imperative to point out, that these observations strongly contradict the rather new interpretation of NM [26] given based on Gd³⁺ moment frustration in GdCrO₃. With increasing concentration of nonmagnetic Y³⁺ ions at the Gd³⁺ site, the density of Gd³⁺ – Gd³⁺ pair correlation will decrease and Gd³⁺ – Y³⁺ and Y³⁺ – Y³⁺ nonmagnetic pair correlations will increase, and hence the Gd³⁺ – Gd³⁺ magnetic correlation will get diluted (decreased). Thus the Gd³⁺ – Gd³⁺

TABLE I. Values of refined parameters obtained through modified Curie-Weiss fit Eq. (6) of the FCC and FCW $M(T)$ data of $\text{Gd}_{1-x}\text{Y}_x\text{CrO}_3$ (for $x = 0, 0.5, 0.67, \text{ and } 0.75$).

x	0		0.5		0.67		0.75		0.80		0.90	
	FCC	FCW	FCC	FCW	FCC	FCW	FCC	FCW	FCC	FCW	FCC	FCW
C	7.8	7.8	3.86	3.86	2.55	2.55	1.93	1.93	1.56	1.56	0.78	0.78
$H_1 \pm 5$	-1350	650	-1610	460	-5190	3960	-4110	2880	-4100	1260	-3880	-2120
$\Theta \pm 0.5$	-17	-1.2	-21.5	-0.39	-10.3	-0.2	-5.2	-0.3	-6	-0.3	-2.4	-1.7
$M(0) \pm 1$	58	-57	50	-37	193	-140	216	-136	202	-51	186	131
$\alpha \pm .1$	1.5	1.5	0.62	0.62	1	1	0.62	0.62	0.62	0.62	0.62	0.62
$\beta \pm .001$	0.053	0.061	0.11	0.12	0.164	0.158	0.19	0.1871	0.20	0.16	0.18	0.198
$T_{N1} \pm 0.5$	169	169	157	157	154	154	147	147	145	145	144	144

moment frustration, if exists at all, will also get decreased. Therefore, if the frustration-based interpretation is correct, the NM effect should decrease with increasing Y^{3+} content. But the experimental observation is just the opposite. Besides this, there are other physical considerations and experimental observations, which go against the possibility of $\text{Gd}^{3+} - \text{Gd}^{3+}$ moment frustration. These are briefly pointed out in the following.

Firstly, the well-established physics of highly localized nature of the *f*-electron wave-function in RE predicts that RE-RE magnetic moment interactions are likely to be very

weak. Hence its ordering or frustration, if at all that happens, it will be at low temperatures. In fact the authors of Ref. [26] themselves estimate the interaction strength to be as small as $\sim 1.66 - 2.37$ K. A moment system, with interaction strength as low as 1.66 K, cannot be expected to remain ordered or exhibit frustration at temperatures ~ 170 K as this is unphysical.

Secondly, if one attributes the occurrence of negative $M_{\text{min-FCC}}$, which is realized during cooling, to the presence of frustration, whose effect keeps increasing on cooling, then the occurrence of negative $M_{\text{min-ZFC/FCW}}$ cannot be even qualitatively explained based on frustration. The ZFC and FCW magnetizations will never decrease from positive to negative during warming up, when the same frustration effect is likely to relax and decrease. Thus the occurrence of negative $M_{\text{min-ZFC/FCW}}$ goes strongly against the frustration based interpretation.

Keeping in view the above discussed facts, the NM effect does not appear to arise due to the said frustration of Gd^{3+} moments, rather it arises due to antiparallel polarization [8,11–13,16,17] of Gd^{3+} moment subsystem against M_C ; decreasing $\text{Gd}^{3+}/\text{Y}^{3+}$ relative concentration will decrease the number of antiparallel polarized Gd^{3+} moments, and hence the NM effect. Thus from this very point of view as well, the occurrence of increasingly high negative value of $M_{\text{min-FCC}}$ appears unusual. However, its one to one correlation with the fitted values of $M(0)$, which increase with Y^{3+} ion concentration, appears to rationalize the issue.

In Eqs. (2) to (4), $M(0)$ is the value of spontaneous magnetization M_C at absolute zero. Since M_C is not directly related with R^{3+} moments, $M(0)$ is expected to be independent of RE magnetization. However, as per the experimental observations summarized in the plots of Fig. 4 and Table I, there is a direct correlation between $M_{\text{min-FCC}}$ and $M_{\text{max-FCC}}$ with $M(0)$ and H_1 .

The physics of the DM interaction [24,25] in systems with superexchange, tells that the canting angle increases with decreasing $\text{M}^{3+}\text{-O-M}^{3+}$ bond angle. Below T_{N1} the Cr^{3+} moments in $\text{Gd}_{1-x}\text{Y}_x\text{CrO}_3$ undergo paramagnetic to $Pb'n'm:\Gamma_4(\mathbf{G}_x, A_y, F_Z; F_Z^R)$ ordered spin configuration, in which the major interaction is \mathbf{G}_x type. It is the canting of this \mathbf{G}_x spin configuration, which gives rise to the small F_z component along the *c* axis of *Pbnm* $\text{Gd}_{1-x}\text{Y}_x\text{CrO}_3$. The net M_C along the *c* axis arises due to the F_z component. Under *Pbnm* setting, the CAFM \mathbf{G}_x is accounted to $\text{Cr}^{3+}\text{-O}_2\text{-Cr}^{3+}$ superexchange pathway. Any change in the $\text{Cr}^{3+}\text{-O}_2\text{-Cr}^{3+}$ bond angle will change the ferromagnetic

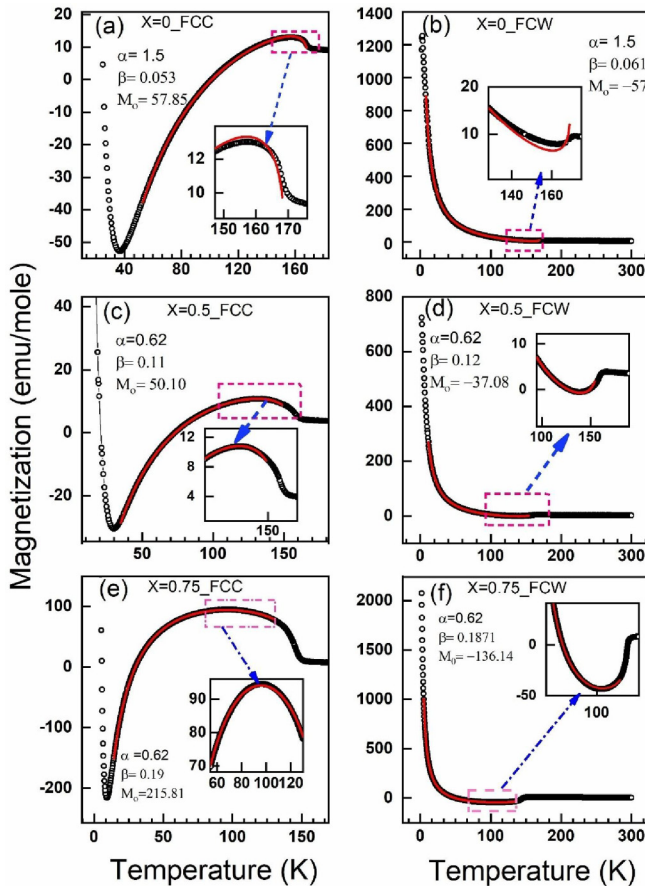


FIG. 5. Modified Curie-Weiss fit of the M-T data of $\text{Gd}_{1-x}\text{Y}_x\text{CrO}_3$ for $x=0, 0.5$ and 0.75 based on Eq. (5) of the text.

component F_z , i.e., the net M_{Cr} along the c axis. From the RT-XRD analysis of $Gd_{1-x}Y_xCrO_3$, as summarized in Tables SM1, SM2 [42], and Fig. 2, it is found that the bond-angle of $Cr^{3+}-O_2-Cr^{3+}$ superexchange pathway decreases with increasing Y^{3+} content. The decreasing bond angle will increase the canting-angle and hence the net M_{Cr} at all temperatures below T_{N1} . This is very much evident from the refined values of spontaneous magnetization $M(0)$, as given in Table I. Since M_{Cr} at any temperature below T_{N1} is larger for higher x , the internal molecular-field, or the exchange-field (H_I) for the $Cr^{3+}-O-Gd^{3+}$ isotropic superexchange will be larger and hence the net Gd^{3+} antiparallel polarization against M_{Cr} will also be larger. From Table I we find that H_I keeps increasing with x and hence the net NM also keeps increasing. Table I shows that irrespective of FCC or FCW, under the given definition of the modified Curie-Weiss behavior, as presented by Eqs. (1) and (5), the Curie-Weiss temperature θ always remains negative. This tells that the isotropic interaction along $Cr^{3+}-O-Gd^{3+}$ pathway always remains AFM.

The NM observed in RE chromates is a low field phenomenon and gets suppressed at fields ~ 2000 Oe. In the $M-H$ isotherms of $Gd_{1-x}Y_xCrO_3$ for $x = 0, 0.5$ and 0.67 , presented in Fig. SM5 [42], we found a systematic decrease in the saturation magnetization (emu/mole) at 2 K, from 170 to 102 to 92 for $x = 0, 0.5$, and 0.67 respectively. This trend of saturation magnetization is commensurate with the decreasing Gd^{3+} content in studied $Gd_{1-x}Y_xCrO_3$ samples. In the $M-H$ isotherms we did not find dM/dH to be negative, so the observed NM does not justify diamagnetism.

Before we proceed further it becomes imperative to discuss about the refined values of α and β given in Table 4. Although the expression $M_{Cr}(T) = M(0) \cdot [1 - (T/T_N)^\alpha]^\beta$ has been successfully used for fitting the $M(T)$ obtained through μ SR measurement and to determine the exponents therein to study the universality class of the magnetic phase transition [45–47], we must emphasize here that in the present case our aim was not to study the universality class of CAFM phase-transition of the Cr-sublattice. Rather, the effort was to just fit the low-field $M(T)$ including the maximum arising under the influence of antiparallel polarization of RE moments below T_{N1} , so that a strong argument can be put in favor of the theory of antiparallel polarization of the RE moments for the observed NM. Despite the very good fit of the low-field $M(T)$ data the refined values for α and β , in principle, cannot be meaningfully associated with any of the universality class. Because at low fields the M_{Cr} measured using bulk technique, is not only a function of temperature but the applied field as well. At a given temperature, for the measured magnetization to be proportional to the spontaneous magnetization in a conventional bulk measurement (VSM or SQUID), it has to be saturated at sufficiently high fields to make it field independent. This is not feasible in the present case. However, μ -SR being a highly local probe, directly measures the spontaneous magnetization itself. The refined values for α and β do show some systematic with the composition in the present samples, but are in general too off from their theoretical predictions, $\alpha \sim 1.5$ for spin-wave excitation and $0.25 \leq \beta \leq 0.5$.

The occurrence of a large hysteresis in the FCC and FCW $M(T)$ s appears alluding the occurrence of a first-order phase transition. While the occurrence of FCC and FCW

$M(T)$ s have been independently discussed in literature quite often but the origin of the continuous sharp rise of the negative magnetization below $T_{min-FCC}$ has been sparsely discussed [17]. In a magnetization study [17] on single crystal $GdCrO_3$ this continuous and sharp rise has in fact been rationalized as a discontinuous magnetization jump within a single temperature-point and has been termed as a temperature-induced magnetization jump (TMJ). Similar to the interpretation of magnetization reversal in for YVO_3 [40], Lin *et al.* [17] too have attributed the TMJ in $GdCrO_3$ to the competing $Cr^{3+} - Cr^{3+}$ spin-canting interactions, the “single-ion anisotropy” and the “DM interaction”.

According to Ref. [17], below T_{N1} a weak-ferromagnetic component M_{Cr} appears due to spin-canting arising due to “single-ion anisotropy” of Cr^{3+} moments. With decreasing temperature M_{Cr} increases and so does the moments of Gd^{3+} subsystem aligned antiparallel to the M_{Cr} under the isotropic $Gd^{3+}-O-Cr^{3+}$ superexchange. Below a certain temperature the Cr^{3+} spin-canting interaction, arising due to “DM interaction”, which is expected to be opposite to that of the “single-ion anisotropy”, dominates the net spin-canting effect and the direction of M_{Cr} gets flipped opposite to the applied field and hence the magnetization due to antiparallel polarized Gd^{3+} subsystem also flips accordingly resulting TMJ. However, looking at the experimental observation of high-temperature shift of TMJ at higher applied fields, the above interpretation [17] of TMJ does not appear to be appropriate. At higher applied fields, the spin-canting due to “single-ion anisotropy” will be boosted and so it will dominate the “DM interaction” down to still lower temperatures, and therefore the TMJ should have shifted to the lower temperatures. But the experimental observation reveals an opposite trend.

The $GdCrO_3$ sample is characteristically different from YVO_3 . In YVO_3 the Y^{3+} ion is nonmagnetic, while in $GdCrO_3$ the Gd^{3+} ion is strongly magnetic. Moreover, there is no direct proof [17] that the two types of Cr^{3+} spin-canting interactions, the “single-ion anisotropy” and the “DM interaction”, coexist in $GdCrO_3$ and that too with opposite signs. Looking at the experimental observations [12,16,17] it appears that the “effect” (the NM) itself is opposing the “cause” (the internal exchange field). The growth of magnetization of the antiparallel aligned Gd^{3+} subsystem, against M_{Cr} , makes the net magnetization opposite to the applied field (H) and hence the net measured magnetization goes negative and the Zeeman energy of the total system becomes high. Thermodynamically this is an unfavorable situation, and therefore, the energetics should have immediately gone down by flipping the net magnetization along the applied field. But such a flip is opposed by the energy-barrier caused by magnetostriction effects, however small it may be. With decreasing temperature the antiparallel magnetization (or polarization) of the Gd^{3+} subsystem keeps increasing, and no sooner the Zeeman-energy overcomes the barrier; the net magnetization of Gd^{3+} subsystem flips along H , making the situation energetically favorable, and remains stable through further FCC below. At still lower temperatures the antisymmetric superexchange through $Gd^{3+}-O-Cr^{3+}$ flips the Cr^{3+} subsystem’s major magnetic order from G_x to G_z and F_z to F_x , resulting into SRPT. The antiparallel polarization of the Gd^{3+} subsystem also follows the SRPT and flips from F_z^{Gd} to F_x^{Gd} . The

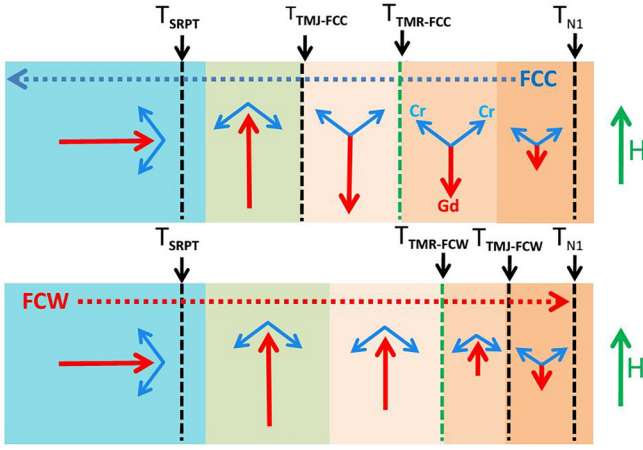


FIG. 6. Temperature evolution of the spin-structure across various magnetic features, like TMR, TMJ, and SRPT, during FCC and FCW under an applied field (H) in $\text{Gd}_{1-x}\text{Y}_x\text{CrO}_3$. It can be noticed that irrespective of FCC or FCW, TMJ always follows TMR.

system now acquires Γ_2 spin structure. The various possible spin arrangements attained by the Gd/Cr magnetic systems, across TMR and TMJ, during FCC and FCW, is depicted in Fig. 6. During FCW, above T_{SRPT} the spin configuration traces back reversibly and the spin configuration of Gd^{3+} subsystem, now oriented parallel to H (but still antiparallel to M_{Cr}), persists till much above the $T_{\text{TMJ-FCC}}$, temperature at which the TMJ appeared the first time during FCC. With increasing temperature the moment of the polarized Gd^{3+} subsystem decreases following the Curie-Weiss law, as expressed by Eq. (5). As it decreases below the magnetization of the canted Cr^{3+} subsystem, which during FCW is now antiparallel to H , magnetization reversal starts at $T_{\text{TMR-FCW}}$. At still higher temperatures, more of the negatively magnetized canted Cr^{3+} subsystem gets exposed to H and the Zeeman-energy again increases, but this time due to oppositely aligned M_{Cr} . During warming the magnetization jump takes place at $T_{\text{TMJ-FCW}}$, while approaching T_{N1} .

The single point magnetization jump feature, as seen for single-crystal GdCrO_3 [17], is not as such realized in polycrystalline GdCrO_3 samples [11,12,16,26]. Instead, a smoothly rising sharp upturn in $M(T)$ is observed. The smoothing is effectively caused by cascaded single magnetization jumps occurring either in different grains/domains or at different individual sites, having distributed $T_{\text{TMJ-FCC}}$ in a given domain of a polycrystalline sample. The distribution of $T_{\text{TMJ-FCC}}$ might be due to distribution in the associated barrier energy, caused by the defect distribution in polycrystalline samples as compared to single crystal. In the present study the distribution width of $T_{\text{TMJ-FCC}}$ is found to range from 5 to 10 K for different $\text{Gd}_{1-x}\text{Y}_x\text{CrO}_3$ samples. The distribution width gets narrower with increasing Y^{3+} . Since the Cr^{3+} concentration remains unchanged, the narrowing of the distribution of $T_{\text{TMJ-FCC}}$ appears to originate from defects associated with the Gd^{3+} magnetic ions. To further probe the nature of distribution of $T_{\text{TMJ-FCC}}$, i.e., whether the distribution is discretely spreads over different domains in a grain or homogeneously distributed over different sites within a domain, we tried di-

viding the system magnetically into two parts as discussed in the following.

Figures 7(a) and 7(b) show the FCC and FCW $M(T)$ s of $\text{Gd}_{1-x}\text{Y}_x\text{CrO}_3$ for $x = 0.75$ measured in slightly different way than the one given in Fig. 3. In Fig. 7(a) the FCC measurement is sharply terminated and FCW started at temperature slightly above (just ~ 1 K) the $T_{\text{FCC-min}}$. We find that the FCW magnetization is exactly reversible to that of the FCC. This is so because above $T_{\text{FCC-min}}$ the whole sample is magnetically uniform. It has antiparallel polarized paramagnetic Gd^{3+} subsystem, which follows Curie-Weiss law. A paramagnetic system does not differentiate between $M(T)$ s measured during cooling or heating. In Fig. 7(b) the FCC was terminated and FCW was started at 6 K, which lies below $T_{\text{FCC-min}}$. As can be noted, the FCW- $M(T)$ is now totally irreversible to FCC- $M(T)$, see inset of Fig. 7(b). Since we have started FCW from an intermediated magnetic situation, the FCW $M(T)$ in Fig. 7(b) stands for coexisting two different “magnetic phases”, one with its Gd^{3+} -subsystem still antiparallel to H and the other, in which the Gd^{3+} subsystem has flipped parallel to H . The magnetic phase with its Gd^{3+} subsystem still antiparallel to H will follow the FCW- $M(T)$ with parameters identical to that of FCC- $M(T)$, and the one with Gd^{3+} subsystem flipped parallel to H , will trace the FCW- $M(T)$ with parameters identical to that of FCW- $M(T)$ represented in Fig. 5(f). If the mass fraction of the “phase” with Gd^{3+} subsystem still antiparallel to H is (p) , then the total FCW $M(T)$ above 6 K can be given by

$$M(T)_{\text{total-FCW}} = pM(T)_{\text{FCC}} + (1-p)M(T)_{\text{FCW}},$$

$$M(T)_{\text{total-FCW}} = \left[\left\{ pM_{0,\text{FCC}} \left[1 - (T/T_{\text{N}})^{\alpha} \right]_{\text{FCC}}^{\beta} \right\} + [C\{(pH_{\text{FCC}} + H)/(T - \theta_{\text{FCC}})\}] \right] + \left[\left\{ (1-p)M_{0,\text{FCW}} \left[1 - (T/T_{\text{N}})^{\alpha} \right]_{\text{FCW}}^{\beta} \right\} + [C\{((1-p)H_{\text{FCW}} + H)/(T - \theta_{\text{FCW}})\}] \right]. \quad (6)$$

There are three possibilities of above discussed coexistence. (1) The net magnetic phase comprise discretely distributed noninteracting domains of the two “phases”, (2) discretely distributed interacting domains of the two “phases” and (3) an all-together different situation comprising individually flipping Gd^{3+} moments occur at homogeneously distributed sites. Figure 7(c) shows the best fit under case (1). This fit to Eq. (6) is clearly too off the experimental data, and hence discarded. The fitting under the second consideration, i.e., interacting discrete domains, results unphysical fit parameters, e.g. the refined value of internal field H_i of both the domains become negative, which is totally against the basic considerations of NM, see Figure SM6 [42], and hence discarded. The fitting under the third consideration of individual flips of polarized Gd^{3+} moments distributed homogeneously over sites, results in proper physical fit to the observed data; see Fig. 7(d). Detail description of the fitting, e.g., the nature of control over the fit parameters of Eq. (6) is given in the SM [42].

The plots in Figs. 4(a), 4(b), and 4(c) show anomalies in the $M_{\text{min-ZFC}}$, $M_{\text{min-FCC}}$ and $M_{\text{max-FCC}}$ variations with x , at $x = 0.5$. This might arise due to the occurrence of possible A-site short-range ordering of Gd^{3+} and Y^{3+} ions, having

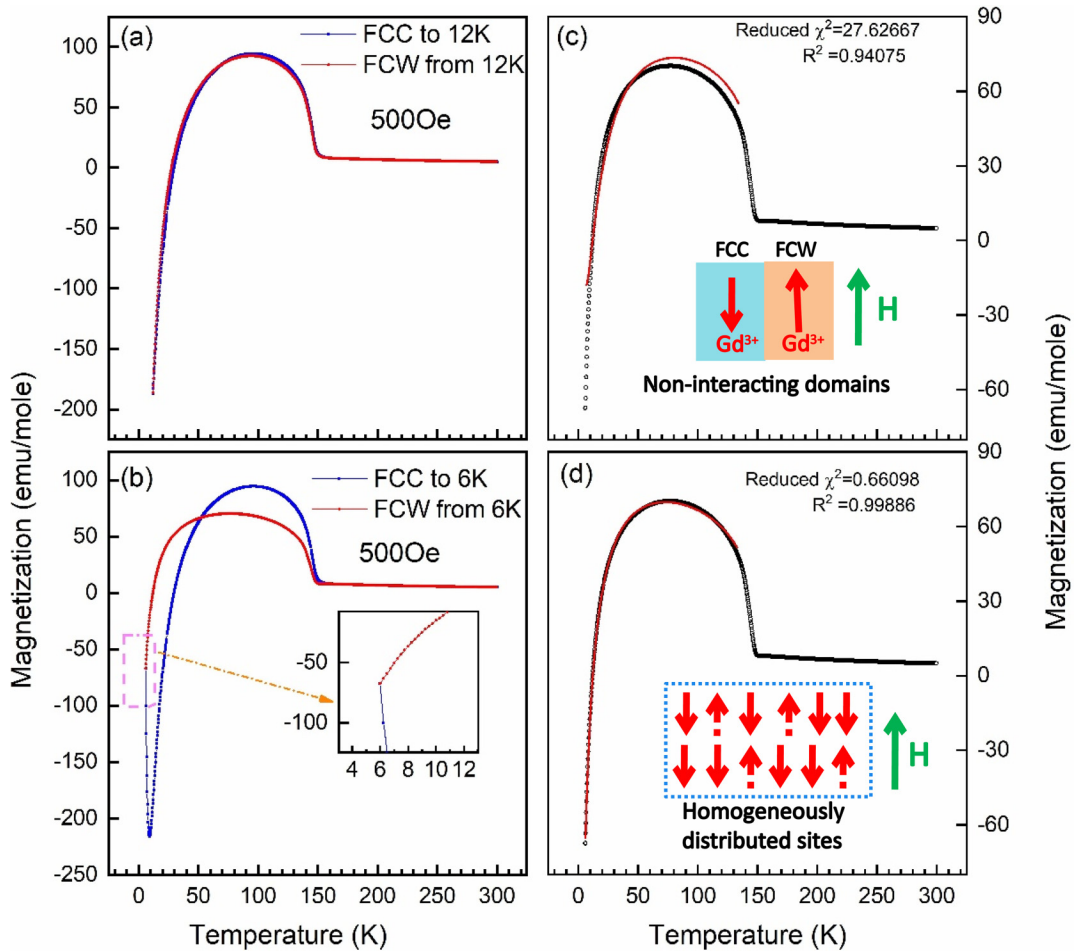


FIG. 7. M-T variation of $Gd_{1-x}Y_xCrO_3$ for $x = 0.75$. It shows (a) that FCW is totally reversible to FCC, while it is measured after reversing the temperature-variation before the TMJ and (b) irreversible, while it is measured after reversing the temperature-variation after TMJ. It clearly depicts that polycrystalline $Gd_{1-x}Y_xCrO_3$ gets split into two different magnetic phases below TMJ. Equation (6) based modified Curie-Weiss fit of the FCW $M(T)$ for $x = 0.75$, (c) while considering noninteracting domains having oppositely flipped Gd^{3+} moments and (d) while considering homogeneously distributed sites with flipped individual Gd^{3+} moments.

different ionic sizes. The diffuse peak intensity arising due to short-range ordering may not be seen in the XRD. However, the ordering is likely to decrease the structural defects, which in turn possibly decreases the barrier-height and enhances the polarizability of Gd^{3+} moments. Let us take M_{Gd_1} as the net magnetization due to polarized Gd^{3+} moments corresponding to $x = 0.4$ and M_{Gd_2} corresponding to $x = 0.5$. Since Cr^{3+} sublattice is not affected much, the M_{Cr} is likely to remain the same for $x = 0.4$ and 0.5 both. Since M_{Gd} arise due to antiparallel polarization against M_{Cr} , usually $M_{Gd} < M_{Cr}$ at temperatures just below T_N . Due to increased polarizability of Gd^{3+} at a given temperature $M_{Gd_2} > M_{Gd_1}$ despite the decreased concentration of Gd^{3+} and therefore the net FCC magnetization close to T_{N1} will be lower for $x = 0.5$ than that of for $x = 0.4$, i.e., $(M_{Cr} - M_{Gd_2}) < (M_{Cr} - M_{Gd_1})$. Thus the $M_{max-FCC}$ will get comparatively suppressed for $x = 0.5$.

At temperatures below TMJ the Gd^{3+} moment subsystem flips parallel to the applied magnetic field and simultaneously compels the M_{Cr} moment subsystem to flip antiparallel to the magnetic field, making the net moment configuration thermodynamically stable. Unlike FCC, the flipped moment

configuration remains stable during ZFC and FCW protocols till quite close to T_{N1} . In this state $M_{Gd} > -M_{Cr}$, i.e., the net ZFC/FCW magnetization ($M_{Gd} - M_{Cr}$) remains positive. With increasing temperature, M_{Gd} decreases much faster, following the Curie-Weiss law, while the M_{Cr} decreases slowly, following $M_{Cr}(T) = M(0)[1 - (T/T_C)^\alpha]^\beta$. Thus at some temperature $M_{Gd} < -M_{Cr}$ and the net ZFC/FCW magnetization now becomes negative. Appearance of NM even during warming is a strong proof that it is the antiparallel polarization of RE moments, which is effective and not the frustration of RE moments. Frustration of RE moments, if at all present, will get relaxed and will not cause NM during warming. Now, as discussed above, due to increased polarizability of Gd^{3+} moments for $x = 0.5$ during ZFC/FCW, $(M_{Gd_2} - M_{Cr}) > (M_{Gd_1} - M_{Cr})$ and hence the $M_{min-ZFC/FCW}$ ($x = 0.5$) $>$ $M_{min-ZFC/FCW}$ ($x = 0.4$). This is what has actually been observed experimentally. Thus the occurrence of above anomalies is fully accountable under the theory of antiparallel polarization of RE moments against M_{Cr} . As proposed in the above, the decreased barrier height will allow the antiparallel polarized Gd^{3+} moments to flip along the applied field (H) at a lower net NM, which will be achieved at slightly

higher temperature itself and therefore $T_{\text{min-FCC}}(x = 0.5) > T_{\text{min-FCC}}(x = 0.4)$.

IV. CONCLUSION

Based on the above described results and discussion on the synthesis, structural and magnetization studies on $\text{Gd}_{1-x}\text{Y}_x\text{CrO}_3$ (for $x = 0 - 0.9$) we conclude that in this compound Gd and Y are fully replaceable for each other due to isostructural nature of the end members, GdCrO_3 and YCrO_3 . The decreasing trend of the lattice parameters with (x) is due to smaller size of Y^{3+} (1.019 Å) ion than that of the Gd^{3+} (1.053 Å). FCC-M(T) revealed the occurrence of negative magnetization, which was found to increase with increasing concentration of nonmagnetic Y^{3+} ions. The sublattice magnetization M_{Cr} of the CAFM ordered Cr subsystem is also found to increase with Y^{3+} ion concentration. This is attributed to the increased canting-angle between the Cr moments arising due to decreasing Cr-O2-Cr bond angle caused by the structural effects arising due to increasing Y^{3+} ion concentration. The increase in NM with increasing Y^{3+} ion concentration is attributed to the increased antiparallel polarization of Gd^{3+} moments against increased M_{Cr} . Our study opposes the interpretation for NM, given based on frustration of Gd^{3+} moments and

strongly testify to the theory of antiparallel polarization of paramagnetic Gd^{3+} moments against uncompensated magnetization of Cr moment subsystem. The occurrence of NM even for ZFC/FCW magnetization uniquely proves the occurrence of antiparallel polarization of RE moments. The TMJ, from negative to positive, has been attributed to the minimization of Zeeman-energy against an energy barrier. A comparative study of the model based fit of $M(T)$, to the modified Curie-Weiss law, clearly indicate that TMJ is an outcome of cascaded flips of individual Gd moments distributed homogeneously over random sites, rather than coherent flips of Gd moments in discreetly distributed magnetic domains.

ACKNOWLEDGMENTS

P.J. and N.P.L. express their sincere gratitude to the Director Prof. A. J. Pal and the Center-Director Dr.V. Sathe UGC-DAE CSR, Indore, for their constant support and encouragement. Authors also acknowledge the National High Magnetic Field Laboratory (NHMFL), USA for conducting some of the magnetization measurements. NHMFL is funded by the National Science Foundation Grant No. DMR-1157490, and the U.S. Department of Energy and the State of Florida.

-
- [1] T. Kimura, T. Goto, H. Shintani, K. Ishizaka, T. Arima, and Y. Tokura, *Nature (London)* **426**, 55 (2003).
- [2] T. Kimura, G. Lawes, T. Goto, Y. Tokura, and A. P. Ramirez, *Phys. Rev. B* **71**, 224425 (2005).
- [3] Y. Tokunaga, S. Iguchi, T. Arima, and Y. Tokura, *Phys. Rev. Lett.* **101**, 097205 (2008).
- [4] T. Yamaguchi and K. Tsushima, *Phys. Rev. B* **8**, 5187 (1973).
- [5] B. Rajeswaran, D. I. Khomskii, A. K. Zvezdin, C. N. R. Rao, and A. Sundaresan, *Phys. Rev. B* **86**, 214409 (2012).
- [6] S. Mahana, B. Rakshit, R. Basu, S. Dhara, B. Joseph, U. Manju, S. D. Mahanti, and D. Topwal, *Phys. Rev. B* **96**, 104106 (2017).
- [7] S. Mahana, U. Manju, P. Nandi, E. Welter, K. R. Priolkar, and D. Topwal, *Phys. Rev. B* **97**, 224107 (2018).
- [8] R. L. White, *J. Appl. Phys.* **40**, 1061 (1969).
- [9] H. Horner and C. M. Varma, *Phys. Rev. Lett.* **20**, 845 (1968).
- [10] T. Yamaguchi, *J. Phys. Chem. Solids* **35**, 479 (1974).
- [11] K. Yoshii, *J. Solid State Chem.* **159**, 204 (2001).
- [12] K. Yoshii, *Mater. Res. Bull.* **47**, 3243 (2012).
- [13] H. J. Zhao, J. Íñiguez, X. M. Chen, and L. Bellaiche, *Phys. Rev. B* **93**, 014417 (2016).
- [14] A. Durán, R. Escamilla, R. Escudero, F. Morales, and E. Verdín, *Phys. Rev. Mater.* **2**, 014409 (2018).
- [15] A. Kumar and S. M. Yusuf, *Phys. Rep.* **556**, 1 (2015).
- [16] S. Biswas and S. Pal, *Rev. Adv. Mater. Sci.* **53**, 206 (2018).
- [17] L. H. Yin, J. Yang, X. C. Kan, W. H. Song, J. M. Dai, and Y. P. Sun, *J. Appl. Phys.* **117**, 133901 (2015).
- [18] N. Kumar and A. Sundaresan, *Solid State Commun.* **150**, 1162 (2010).
- [19] Y. Cao, S. Cao, W. Ren, Z. Feng, S. Yuan, B. Kang, B. Lu, and J. Zhang, *Appl. Phys. Lett.* **104**, 232405 (2014).
- [20] Y. K. Jeong, J.-H. Lee, S.-J. Ahn, and H. M. Jang, *Solid State Commun.* **152**, 1112 (2012).
- [21] A. Kimel, B. Ivanov, R. Pisarev, P. Usachev, A. Kirilyuk, and T. Rasing, *Nat. Phys.* **5**, 727 (2009).
- [22] S. Terkhi, S. Bentata, Z. Aziz, T. Lantri, and B. Abbar, *Indian J. Phys.* **92**, 847 (2018).
- [23] M. Shao, S. Cao, S. Yuan, J. Shang, B. Kang, B. Lu, and J. Zhang, *Appl. Phys. Lett.* **100**, 222404 (2012).
- [24] I. Dzyaloshinsky, *Phys. Chem. Solids* **4**, 241 (1958).
- [25] T. Moriya, *Phys. Rev. Lett.* **4**, 228 (1960).
- [26] M. Tripathi, R. J. Choudhary, and D. M. Phase, *Phys. Rev. B* **99**, 014422 (2019).
- [27] T. Sau, S. Sharma, P. Yadav, R. Baumbach, T. Siegrist, A. Banerjee, and N. P. Lalla, *Phys. Rev. B* **106**, 064413 (2022).
- [28] Ya. B. Bazaliy, L. T. Tsybmal, G. N. Kakazei, A. I. Izotov, and P. E. Wigen, *Phys. Rev. B* **69**, 104429 (2004).
- [29] T. Chakraborty and S. Elizabeth, *J. Magn. Magn. Mater* **462**, 78 (2018).
- [30] T. Hamsaki, M. Arai, T. Yokoo, S. Ohara, and I. Sakamoto, *J. Magn. Magn. Mater* **272-276**, e465 (2004).
- [31] G. R. HariPriya, H. S. Nair, R. Pradheesh, S. Rayaprol, V. sirugui, D. Singh, R. Venkatesh, V. Ganesan, K. Setupathi, and V. Sankarnarayanan, *J. Phys.: Condens. Matter* **29**, 475804 (2017).
- [32] R. M. Hornreich, *J. Magn. Magn. Mater.* **7**, 280 (1978).
- [33] M. A. McGuire, R. P. Hermann, A. S. Sefat, B. C. Sales, R. Jin, D. Mandrus, F. Grandjean, and G. J. Long, *New J. Phys.* **11**, 025011 (2009).
- [34] L. M. Levinson, M. Luban, and S. Shtrikman, *Phys. Rev.* **187**, 715 (1969).

- [35] G. Gorodetsky, R. Hornreich, S. Shaft, B. Sharon, A. Shaulov, and B. M. Wanklyn, *Phys. Rev. B* **16**, 515 (1977).
- [36] Y. Imry and M. Wortis, *Phys. Rev. B* **19**, 3580 (1979).
- [37] M. Taheri and F. S. Raavi, *Phys. Rev. B* **93**, 104414 (2016).
- [38] A. N. Pirogov, S. G. Bogdanov, Y. N. Choi, E. V. Rozenfeld, V. Choi, and Yu. N. Skryabin, *Solid State Phenomena* **168-169**, 138 (2011).
- [39] A. H. Cooke, D. M. Martin, and M. R. Wells, *J. Phys. C* **7**, 3133 (1974).
- [40] Y. Ren, T. T. M. Palstra, D. I. Khomskii, A. A. Nugroho, A. A. Menovsky, and G. A. Sawatzky, *Phys. Rev. B* **62**, 6577 (2000).
- [41] M. Dusek Petricek and L. Palatinus, *Z. Kristallogr.* **229**, 345 (2014).
- [42] See Supplemental Material at <http://link.aps.org/supplemental/10.1103/PhysRevB.109.094410> for looking into (a) all Rietveld refined RT-XRD data and refined structural parameters, (b) full view of the M(T)s corresponding to all the studies samples, (c) Modified Curie-Wiess fit of all the M(T)s, as per Eqs. (1) and (5) of the main text and the details of fitting of FCW-M(T) data of x0.75 using Eq. (6). The Supplemental Material also contains Refs. [48,49].
- [43] R. D. Shannon, *Acta Cryst. A* **32**, 751 (1976).
- [44] C. N. R. Rao, *Encyclopedia of Physical Science and Technology*, 3rd ed., edited by R. A. Meyers (Academic Press, California, 2001).
- [45] M. Czapla, R. Pelka, P. M. Zielinski, A. Budziak, M. Balanda, M. Makarewicz, A. Pacyna, and T. Wasiutynski, *Phys. Rev. B* **82**, 094446 (2010).
- [46] P. J. Baker, T. Lancaster, I. Franke, W. Hayes, S. J. Blundell, F. L. Pratt, P. Jain, Z.-M. Wang, and M. Kurmoo, *Phys. Rev. B* **82**, 012407 (2010).
- [47] R. Pełka, M. Czapla, P. M. Zieliński, M. Fitta, M. Bałanda, D. Pinkowicz, F. L. Pratt, M. Mihalik, J. Przewoźnik, A. Amato, B. Sieklucka, and T. Wasiutyński, *Phys. Rev. B* **85**, 224427 (2012).
- [48] L. F. Mendivil, J. Alvarado Rivera, E. Verdín, J. A. Díaz, J. Mata, A. Conde, and A. Durán, *Appl. Phys. A* **126**, 574 (2020).
- [49] B. Dalal, B. Sarkar, S. Rayaprol, M. Das, V. Siruguri, P. Mandal, and S. K. De, *Phys. Rev. B* **101**, 144418 (2020).